Available online at www.sciencedirect.com
ScienceDirect
Journal of Sound and Vibration 299 (2007) 373–387
JOURNAL OF SOUND AND VIBRATION
www.elsevier.com/locate/jsvi

Short Communication

Vibration analyses of an inclined flat plate subjected to moving loads

Jia-Jang Wu*

Department of Marine Engineering, National Kaohsiung Marine University, No. 142, Hai-Chuan Road, Nan-Tzu, Kaohsiung 811, Taiwan, Republic of China

Received 28 May 2006; received in revised form 3 July 2006; accepted 9 July 2006
Available online 11 September 2006

Abstract

The object of this paper is to present a moving mass element so that one may easily perform the dynamic analysis of an inclined plate subjected to moving loads with the effects of inertia force, Coriolis force and centrifugal force considered. To this end, the mass, damping and stiffness matrices of the moving mass element, with respect to the local coordinate system, are derived first by using the principle of superposition and the definition of shape functions. Next, the last property matrices of the moving mass element are transformed into the global coordinate system and combined with the property matrices of the inclined plate itself to determine the effective overall property matrices and the instantaneous equations of motion of the entire vibrating system. Because the property matrices of the moving mass element have something to do with the instantaneous position of the moving load, both the property matrices of the moving mass element and the effective overall ones of the entire vibrating system are time-dependent. At any instant of time, solving the instantaneous equations of motion yields the instantaneous dynamic responses of the inclined plate. For validation, the presented technique is used to determine the dynamic responses of a horizontal pinned–pinned plate subjected to a moving load and a satisfactory agreement with the existing literature is achieved. Furthermore, extensive studies on the inclined plate subjected to moving loads reveal that the influences of moving-load speed, inclined angle of the plate and total number of the moving loads on the dynamic responses of the inclined plate are significant in most cases, and the effects of Coriolis force and centrifugal force are perceptible only in the case of higher moving-load speed.

1. Introduction

The reports concerning the dynamic behaviour of *horizontal* plates due to moving or stationary dynamic loads are abundant [1–13], however, the literature regarding those of *inclined* plates subjected to moving loads is limited. Since the existing technique for the moving-load-induced vibrations of *horizontal* plates cannot be directly applied to the title problem, this paper aims to extend the technique for those of one-dimensional inclined beams [14] to the two-dimensional inclined plates, so that the dynamic characteristics of the inclined

*Tel.: +886 7 8100888x5230; fax: +886 6 2808458.
E-mail address: jjangwu@mail.nkmu.edu.tw.

0022-460X/$ - see front matter © 2006 Elsevier Ltd. All rights reserved.
doi:10.1016/j.jsv.2006.07.002

plates undergoing moving loads, with the effects of inertia force, Coriolis force and centrifugal force considered, can be easily determined.

First, under the assumption that each moving load is always in contact with the inclined plate, the property matrices of *moving mass element*, with respect to the local (xyz) coordinates of the plate element on which the moving load applies, are derived. Next, the last property matrices are transformed into the ones with respect to the global ($\bar{x}\bar{y}\bar{z}$) coordinates of the entire vibrating system and added to the overall mass, damping and stiffness matrices of the inclined plate itself. Thus, the effects of inertia force, Coriolis force and centrifugal force, induced by the moving load, can be easily taken into account. Finally, the equations of motion are solved to yield the dynamic responses of the inclined plate due to moving loads, and the influence of some factors relating to the title problem are investigated.

2. Moving mass element

With respect to the local coordinates xyz of the inclined plate element on which the moving concentrated load with mass m_c is located, as shown in Fig. 1, the in-plane forces (F_{Ix} and F_{Iy}) and out-of-plane force (F_{Iz}) at the contact point i induced by m_c, due to vibration and curvature of the plate element, are, respectively, given by [6]

$$F_{Ix} = m_c \ddot{u}_{ix}, \tag{1a}$$

$$F_{Iy} = m_c \ddot{u}_{iy}, \tag{1b}$$

$$\begin{aligned} F_{Iz} = m_c[&V_{cx}^2 u_{iz}^{xx} + 2V_{cx}V_{cy}u_{iz}^{xy} + 2V_{cx}\dot{u}_{iz}^{x} + 2V_{cy}\dot{u}_{iz}^{y} \\ &+ V_{cy}^2 u_{iz}^{yy} + \dot{V}_{cx}u_{iz}^{x} + \dot{V}_{cy}u_{iz}^{y} + \ddot{u}_{iz}], \end{aligned} \tag{1c}$$

where u_{ix}, u_{iy} and u_{iz} are the displacements of point i in x, y and z directions, while V_{cx} and V_{cy} are the velocities of the moving load m_c in x and y directions, respectively. The superscripts x, y and the overhead dot represent the derivatives with respect to x, y and time t, respectively.

The equivalent nodal forces at the four nodes of the plate element due to the last three inertial forces, F_{Ix}, F_{Iy} and F_{Iz}, at point i, are given by [15,16]

$$f_k = \phi_k F_{Ix} \quad (k = 1, 7, 13, 19), \quad f_k = \phi_k F_{Iy} \quad (k = 2, 8, 14, 20), \quad f_k = 0 \quad (k = 6, 12, 18, 24), \tag{2a}$$

$$f_k = \phi_k F_{Iz} \quad (k = 3, 4, 5, 9, 10, 11, 15, 16, 17, 21, 22, 23), \tag{2b}$$

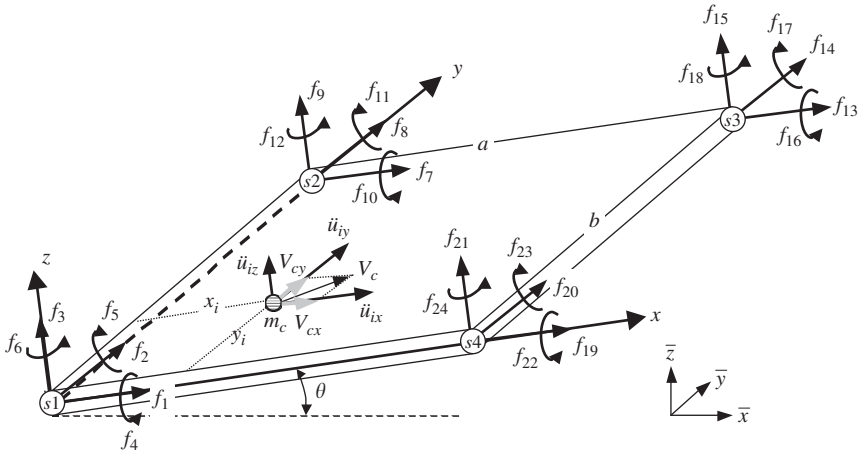

Fig. 1. Equivalent nodal forces of the inclined plate element due to a moving mass m_c.

where ϕ_k (k =1–24) are the shape functions, and those associated with the non-zero equivalent nodal forces are given by [12,16]

$$\begin{aligned}
&\phi_1 = \phi_2 = (1-\varsigma)(1-\eta), \quad \phi_3 = (1+2\varsigma)(1-\varsigma)^2(1+2\eta)(1-\eta)^2,\\
&\phi_4 = (1+2\varsigma)(1-\varsigma)^2\eta(1-\eta)^2 b, \quad \phi_5 = -(1-\varsigma)^2\varsigma(1+2\eta)(1-\eta)^2 a, \quad \phi_7 = \phi_8 = (1-\varsigma)\eta,\\
&\phi_9 = (1+2\varsigma)(1-\varsigma)^2(3-2\eta)\eta^2, \quad \phi_{10} = -(1+2\varsigma)(1-\varsigma)^2(1-\eta)\eta^2 b,\\
&\phi_{11} = -\varsigma(1-\varsigma)^2(3-2\eta)\eta^2 a, \quad \phi_{13} = \phi_{14} = \varsigma\eta, \quad \phi_{15} = (3-2\varsigma)\varsigma^2(3-2\eta)\eta^2,\\
&\phi_{16} = -(3-2\varsigma)\varsigma^2(1-\eta)\eta^2 b, \quad \phi_{17} = (1-\varsigma)\varsigma^2(3-2\eta)\eta^2 a, \quad \phi_{19} = \phi_{20} = \varsigma(1-\eta),\\
&\phi_{21} = (3-2\varsigma)\varsigma^2(1+2\eta)(1-\eta)^2, \quad \phi_{22} = (3-2\varsigma)\varsigma^2\eta(1-\eta)^2 b, \quad \phi_{23} = (1-\varsigma)\varsigma^2(1+2\eta)(1-\eta)^2 a, \qquad (3a)
\end{aligned}$$

$$\varsigma = \frac{x_i}{a}, \quad \eta = \frac{y_i}{b}. \qquad (3b)$$

In the last expressions, a and b, respectively, represent the width and length of the plate element (see Fig. 1), while x_i and y_i represent the x and y coordinates of the moving mass m_c, respectively.

Based on the definition of shape functions [16], one obtains

$$u_{ix} = \phi_1 u_1 + \phi_7 u_7 + \phi_{13} u_{13} + \phi_{19} u_{19}, \qquad (4a)$$

$$u_{iy} = \phi_2 u_2 + \phi_8 u_8 + \phi_{14} u_{14} + \phi_{20} u_{20}, \qquad (4b)$$

$$\begin{aligned}
u_{iz} = {} & \phi_3 u_3 + \phi_4 u_4 + \phi_5 u_5 + \phi_9 u_9 + \phi_{10} u_{10} + \phi_{11} u_{11}\\
& + \phi_{15} u_{15} + \phi_{16} u_{16} + \phi_{17} u_{17} + \phi_{21} u_{21} + \phi_{22} u_{22} + \phi_{23} u_{23}, \qquad (4c)
\end{aligned}$$

where u_i ($i = 1, 2, \ldots$) are the nodal displacements of the plate element.

Introducing Eqs. (1) and (4) into Eq. (2), and writing the resulting expressions in matrix form, one obtains

$$\{f\} = [m]\{\ddot{u}\} + [c]\{\dot{u}\} + [k]\{u\}, \qquad (5)$$

$$\{f\} = [f_1 \quad f_2 \quad \cdots \quad f_{23} \quad f_{24}]^{\mathrm{T}}, \quad \{\ddot{u}\} = [\ddot{u}_1 \quad \ddot{u}_2 \quad \cdots \quad \ddot{u}_{23} \quad \ddot{u}_{24}]^{\mathrm{T}},$$

$$\{\dot{u}\} = [\dot{u}_1 \quad \dot{u}_2 \quad \cdots \quad \dot{u}_{23} \quad \dot{u}_{24}]^{\mathrm{T}}, \quad \{u\} = [u_1 \quad u_2 \quad \cdots \quad u_{23} \quad u_{24}]^{\mathrm{T}}. \qquad (6)$$

In Eq. (5), all the coefficients of $[m]_{24\times 24}$, $[c]_{24\times 24}$ and $[k]_{24\times 24}$ are equal to zero except

$$m_{\alpha\beta} = m_c\phi_\alpha\phi_\beta \quad (\alpha,\beta = 1,7,13,19), \quad m_{\alpha\beta} = m_c\phi_\alpha\phi_\beta \quad (\alpha,\beta = 2,8,14,20), \qquad (7a)$$

$$m_{\alpha\beta} = m_c\phi_\alpha\phi_\beta \quad (\alpha,\beta = 3,4,5,9,10,11,15,16,17,21,22,23), \qquad (7b)$$

$$c_{\alpha\beta} = 2m_c V_{cx}\phi_\alpha\phi_\beta^x + 2m_c V_{cy}\phi_\alpha\phi_\beta^y \quad (\alpha,\beta = 3,4,5,9,10,11,15,16,17,21,22,23), \qquad (7c)$$

$$\begin{aligned}
k_{\alpha\beta} = {} & m_c V_{cx}^2\phi_\alpha\phi_\beta^{xx} + 2m_c V_{cx}V_{cy}\phi_\alpha\phi_\beta^{xy} + m_c V_{cy}^2\phi_\alpha\phi_\beta^{yy} + m_c\dot{V}_{cx}\phi_\alpha\phi_\beta^x + m_c\dot{V}_{cy}\phi_\alpha\phi_\beta^y\\
& (\alpha,\beta = 3,4,5,9,10,11,15,16,17,21,22,23). \qquad (7d)
\end{aligned}$$

In Eq. (5), $[m]$, $[c]$ and $[k]$ are, respectively, the mass, damping and stiffness matrices of *moving mass element* with effects of inertia force, Coriolis force and centrifugal force induced by the moving mass m_c considered. From Eq. (7) and the shape functions, ϕ_k (k =1–24), one finds that the last property matrices are time-dependent.

3. Transformation of moving mass element

From Ref. [17], one can obtain the relation between the local nodal displacements u_i (i =1–24) and the global ones $\bar{u}_i$ (i =1–24) of the plate element on which the moving concentrated mass m_c applies

$$\{u\} = [T]\{\bar{u}\}, \qquad (8)$$

where

$$\{u\} = [\,u_1 \quad u_2 \quad \ldots \quad u_{23} \quad u_{24}\,]^{\mathrm{T}}, \quad \{\bar{u}\} = [\,\bar{u}_1 \quad \bar{u}_2 \quad \ldots \quad \bar{u}_{23} \quad \bar{u}_{24}\,]^{\mathrm{T}}, \tag{9a}$$

$$[T] = \lceil \lambda \;\; \lambda \;\; \lambda \;\; \lambda \;\; \lambda \;\; \lambda \;\; \lambda \;\; \lambda \rfloor \tag{9b}$$

with

$$\lambda = \begin{bmatrix} \alpha_x & \beta_x & \gamma_x \\ \alpha_y & \beta_y & \gamma_y \\ \alpha_z & \beta_z & \gamma_z \end{bmatrix},$$

$$\alpha_x = \frac{\Delta x}{L}, \quad \beta_x = \frac{\Delta y}{L}, \quad \gamma_x = \frac{\Delta z}{L}, \quad \alpha_y = \frac{B_1}{B}, \quad \beta_y = \frac{B_2}{B}, \quad \gamma_y = \frac{B_3}{B},$$

$$\alpha_z = \beta_x\gamma_y - \gamma_x\beta_y, \quad \beta_z = \gamma_x\alpha_y - \alpha_x\gamma_y, \quad \gamma_z = \alpha_x\beta_y - \beta_x\alpha_y,$$

$$\Delta x = \bar{x}_{s4} - \bar{x}_{s1}, \quad \Delta y = \bar{y}_{s4} - \bar{y}_{s1}, \quad \Delta z = \bar{z}_{s4} - \bar{z}_{s1},$$

$$L = \sqrt{\Delta x^2 + \Delta y^2 + \Delta z^2},$$

$$B_1 = A_2\Delta z - A_3\Delta y, \quad B_2 = A_3\Delta x - A_1\Delta z, \quad B_3 = A_1\Delta y - A_2\Delta x, \quad B = \sqrt{B_1^2 + B_2^2 + B_3^2},$$

$$A_1 = \Delta y\Delta z_s - \Delta z\Delta y_s, \quad A_2 = \Delta z\Delta x_s - \Delta x\Delta z_s, \quad A_3 = \Delta x\Delta y_s - \Delta y\Delta x_s,$$

$$\Delta x_s = \bar{x}_{s2} - \bar{x}_{s1}, \quad \Delta y_s = \bar{y}_{s2} - \bar{y}_{s1}, \quad \Delta z_s = \bar{z}_{s2} - \bar{z}_{s1}. \tag{10}$$

In Eq. (9b), the symbol $\lceil\,\rfloor$ denotes a diagonal matrix and in Eq. (10), $\bar{x}_k, \bar{y}_k$ and $\bar{z}_k$, respectively, represent the global $\bar{x}, \bar{y}$, and $\bar{z}$ coordinates for node k ($k = s1, s2, s4$) of the plate element (see Fig. 1), while $[T]$ is the transformation matrix between the local coordinates xyz and the global coordinates $(\bar{x}\bar{y}\bar{z})$.

Similarly, the relationship between the nodal forces in local coordinates xyz, f_i ($i = 1-24$), and those in global coordinates $(\bar{x}\bar{y}\bar{z})$, $\bar{f}_i$ ($i = 1-24$), is given by

$$\{f\} = [T]\{\bar{f}\} = [T][\bar{f}_1 \quad \bar{f}_2 \quad \cdots \quad \bar{f}_{23} \quad \bar{f}_{24}\,]^{\mathrm{T}}. \tag{11}$$

Time derivatives of Eq. (8) lead to

$$\{\dot{u}\} = [T]\{\dot{\bar{u}}\}, \quad \{\ddot{u}\} = [T]\{\ddot{\bar{u}}\}. \tag{12}$$

Introducing Eqs. (8), (11) and (12) into Eq. (5) leads to

$$\{\bar{f}\} = [\bar{m}]\{\ddot{\bar{u}}\} + [\bar{c}]\{\dot{\bar{u}}\} + [\bar{k}]\{\bar{u}\}, \tag{13a}$$

where

$$[\bar{m}] = [T]^{\mathrm{T}}[m][T], \tag{13b}$$

$$[\bar{c}] = [T]^{\mathrm{T}}[c][T], \tag{13c}$$

$$[\bar{k}] = [T]^{\mathrm{T}}[k][T]. \tag{13d}$$

In Eqs. (13b)–(13d), $[\bar{m}], [\bar{c}]$ and $[\bar{k}]$ are, respectively, the mass, damping and stiffness matrices of the *moving mass element* with respect to the global $(\bar{x}\bar{y}\bar{z})$ coordinates of the entire vibrating system. Because $[m]$, $[c]$ and $[k]$ are time-variant, so are $[\bar{m}], [\bar{c}]$ and $[\bar{k}]$.

4. Equations of motion of the entire vibrating system

The equations of motion for a damped inclined plate undergoing moving loads take the form

$$[\hat{M}]\{\ddot{\hat{q}}\} + [\hat{C}]\{\dot{\hat{q}}\} + [\hat{K}]\{\hat{q}\} = \{\hat{F}\}, \tag{14}$$

where $[\hat{M}], [\hat{C}]$ and $[\hat{K}]$ are the *instantaneous* overall mass, damping and stiffness matrices, respectively; $\{\ddot{\hat{q}}\}$, $\{\dot{\hat{q}}\}$ and $\{\hat{q}\}$ are the acceleration, velocity and displacement vectors, respectively; while $\{\hat{F}\}$ is the *instantaneous* external force vector.

5. Instantaneous overall property matrices of the entire vibrating system

The *instantaneous* overall mass, damping and stiffness matrices, $[\hat{M}], [\hat{C}]$ and $[\hat{K}]$, appearing in Eq. (14) are obtained by adding the mass, damping and stiffness matrices of the *moving mass element*, $[\bar{m}], [\bar{c}]$ and $[\bar{k}]$, to the overall mass, damping and stiffness matrices of the inclined plate itself, $[M_p], [C_p]$ and $[K_p]$, i.e.,

$$[\hat{M}]_{n\times n} = [M_p]_{n\times n} + [\bar{m}]_{24\times 24},\ \ [\hat{C}]_{n\times n} = [C_p]_{n\times n} + [\bar{c}]_{24\times 24},\ \ [\hat{K}]_{n\times n} = [K_p]_{n\times n} + [\bar{k}]_{24\times 24}, \tag{15}$$

where

$$\hat{M}_{ij} = M_{p,ij}, \quad \hat{C}_{ij} = C_{p,ij}, \quad \hat{K}_{ij} = K_{p,ij} \quad (i,j = 1{-}n), \tag{16}$$

except that

$$\hat{M}_{s_i s_j} = M_{p,s_i s_j} + \bar{m}_{ij}, \quad \hat{C}_{s_i s_j} = C_{p,s_i s_j} + \bar{c}_{ij}, \quad \hat{K}_{s_i s_j} = K_{p,s_i s_j} + \bar{k}_{ij} \quad (i,j = 1{-}24). \tag{17}$$

In the last expressions, n represents the total degree of freedom (dof) of the entire vibrating system and the subscripts s_i (i =1–24), respectively, represent the numberings for the 24 dof of the four nodes of the plate element on which the moving load m_c applies at time t. The overall damping matrix $[C_p]$ of the plate itself is determined by using the theory of Rayleigh damping [18]

$$[C_p] = \varepsilon_1[\hat{M}] + \varepsilon_2[\hat{K}], \tag{18a}$$

$$\varepsilon_1 = \frac{2\Omega_i\Omega_j(\xi_i\Omega_j - \xi_j\Omega_i)}{\Omega_j^2 - \Omega_i^2}, \tag{18b}$$

$$\varepsilon_2 = \frac{2(\xi_j\Omega_j - \xi_i\Omega_i)}{\Omega_j^2 - \Omega_i^2}, \tag{18c}$$

where ξ_i and ξ_j are damping ratios corresponding to any two natural frequencies of the entire vibrating system, Ω_i and Ω_j.

6. Equivalent nodal forces and overall external force vector

Referring to Fig. 1, one has the external force vector $\vec{P}$ due to the moving mass m_c

$$\vec{P} = P_x\vec{i} + P_y\vec{j} + P_z\vec{k} \tag{19}$$

with

$$P_x = -m_c g\gamma_x, \quad P_y = -m_c g\gamma_y, \quad P_z = -m_c g\gamma_z, \tag{20}$$

where $\vec{i}$, $\vec{j}$ and $\vec{k}$ are, respectively, the unit vectors in x, y and z directions, γ_x, γ_y and γ_z are given by Eq. (10) and g is the acceleration of gravity.

For the finite element analysis, the last force vector $\vec{P}$ must be replaced by an *equivalent nodal force vector*

$$\{f^{(s)}\} = [f_1^{(s)} \quad f_2^{(s)} \quad \cdots \quad f_{23}^{(s)} \quad f_{24}^{(s)}]^{\mathrm{T}}. \tag{21}$$

In Eq. (21), the non-zero coefficients are given by

$$f_k^{(s)} = \phi_k P_x \quad (k = 1, 7, 13, 19), \tag{22a}$$

$$f_k^{(s)} = \phi_k P_y \quad (k = 2, 8, 14, 20), \tag{22b}$$

$$f_k^{(s)} = \phi_k P_z \quad (k = 3, 4, 5, 9, 10, 11, 15, 16, 17, 21, 22, 23), \tag{22c}$$

where the superscript s refers to the numbering of the plate element.

Eq. (21) denotes the nodal force vector in local xyz coordinates, therefore, the corresponding one in global $(\bar{x}\bar{y}\bar{z})$ coordinates is given by

$$\{\bar{f}^{(s)}\} = [\bar{f}_1^{(s)} \quad \bar{f}_2^{(s)} \quad \dots \quad \bar{f}_{23}^{(s)} \quad \bar{f}_{24}^{(s)}]^{\mathrm{T}} = [T]^{-1}\{f^{(s)}\} = [T]^{\mathrm{T}}\{f^{(s)}\}. \tag{23}$$

Since all nodal forces of the entire vibrating system are equal to zero except those at the four nodes of the sth plate element on which the moving mass m_c applies, the overall external force vector $\{\hat{F}\}$ in Eq. (14) takes the form

$$\{\hat{F}\} = [0 \quad \dots \quad \bar{f}_1^{(s)} \quad \bar{f}_2^{(s)} \quad \dots \quad \bar{f}_{23}^{(s)} \quad \bar{f}_{24}^{(s)} \quad \dots \quad 0]^{\mathrm{T}}, \tag{24}$$

where $\bar{f}_i^{(s)}$ are the s_i coefficients of $\{\hat{F}\}$ with s_i $(i = 1\text{–}24)$ denoting the numberings for the 24 dof of the plate element.

7. Dynamic responses of the inclined plate due to moving loads

First, the finite element model of the inclined plate is established and the natural frequencies and mode shapes of the inclined plate itself are calculated by using the Jacobi method [18]. Next, the *instantaneous* mass, damping and stiffness matrices, $[\bar{m}]$, $[\bar{c}]$ and $[\bar{k}]$, of the *moving mass element* are calculated using Eq. (13), and then the *instantaneous* overall mass, damping and stiffness matrices, $[\hat{M}], [\hat{C}]$ and $[\hat{K}]$, and the *instantaneous* overall force vector $\{\hat{F}\}$ of the entire vibrating system at time t are determined using Eqs. (15)–(18) and Eqs. (19)–(24), respectively. Finally, the Newmark direct integration method [18] is used to solve the equations of motion, Eq. (14), to determine the dynamic responses of the inclined plate due to moving loads at time t. Repeating the last steps, one may obtain the responses of the vibrating system at time instants $t = t + j \times \Delta t$ $(j = 1, 2, 3, \dots,$ etc.).

8. Numerical results

The dimensions and physical properties of the pinned–pinned (P–P) rectangular plate studied are (see Fig. 2 with the two opposite sides, AB and CD, pinned): length $L_{px} = 1.0\,\mathrm{m}$, width $L_{py} = 0.5\,\mathrm{m}$, thickness $L_{pz} = 0.01\,\mathrm{m}$, mass density $\rho_p = 7820\,\mathrm{kg/m^3}$, modulus of elasticity $E_p = 206.8\,\mathrm{GN/m^2}$ and Poisson's ratio $v = 0.29$. The entire plate is modelled with 32 identical $0.125\,\mathrm{m} \times 0.125\,\mathrm{m}$ rectangular plate elements and

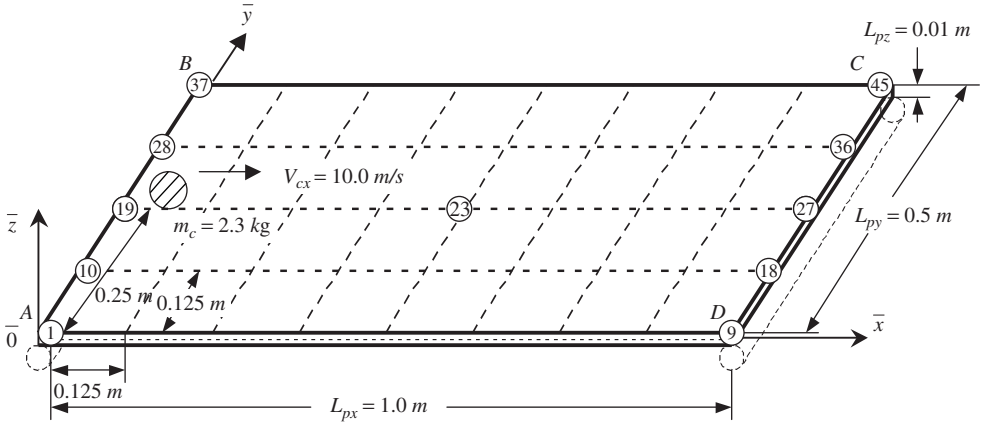

Fig. 2. A horizontal pinned–pinned rectangular plate subjected to a load with mass $m_c = 2.3\,\mathrm{kg}$ moving from side AB to side CD with a constant speed $V_{cx} = 10.0\,\mathrm{m/s}$.

45 nodes. All results are obtained with acceleration of gravity $g = 9.81\,\mathrm{m/s^2}$, time interval $\Delta t = 0.001\,\mathrm{s}$, damping ratios $\xi_1 = \xi_2 = 0.005$ (corresponding to natural frequencies Ω_1 and Ω_2).

8.1. Validation

In this subsection, the dynamic analysis of the *horizontal* P–P plate (inclined angle $\theta = 0^\circ$) subjected to a moving load with mass $m_c = 2.3\,\mathrm{kg}$ moving from side AB to side CD with a constant speed $V_{cx} = 10.0\,\mathrm{m/s}$

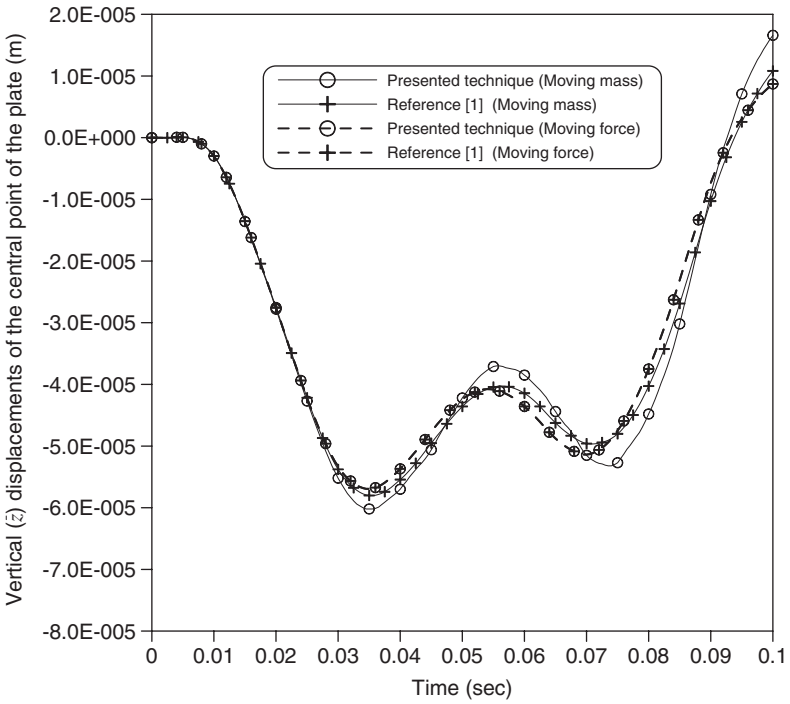

Fig. 3. Time histories for the vertical ($\bar{z}$) central displacements of the horizontal pinned–pinned (P–P) plate under a moving load with mass $m_c = 2.3\,\mathrm{kg}$ and $V_{cx} = 10.0\,\mathrm{m/s}$.

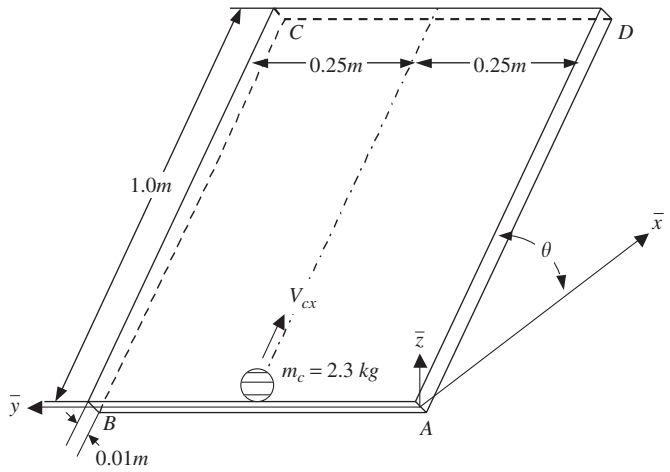

Fig. 4. An inclined P–P plate subjected to a concentrated load $m_c = 2.3\,\mathrm{kg}$ moving from lower-side AB to upper-side CD of the plate with a constant speed V_{cx}.

(see Fig. 2) is performed. Fig. 3 shows the time histories for the vertical ($\bar{z}$) displacements of the central point of the horizontal plate. In which, the solid curve with circles (—○—) and dashed curve with circles (--○--), respectively, represent the responses due to a moving mass and a moving force obtained from this paper, while the solid curve with crosses (—+—) and dashed curve with crosses (--+--),

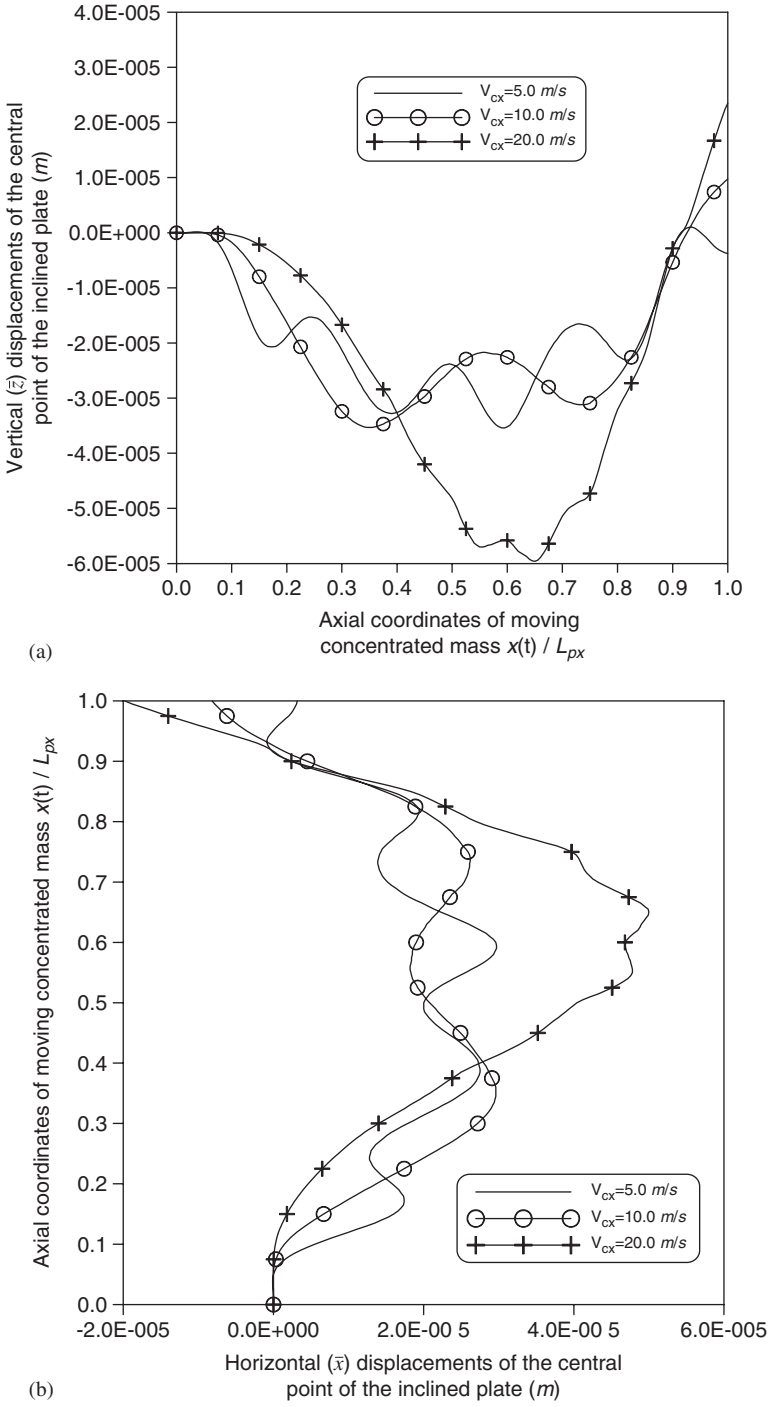

Fig. 5. Influence of moving speed (V_{cx}) on (a) vertical ($\bar{z}$) and (b) horizontal ($\bar{x}$) central displacements of the inclined plate ($\theta = 40^{\circ}$) due to a moving load with mass $m_c = 2.3$ kg and constant moving speeds $V_{cx} = 5.0$, 10.0 and 20.0 m/s.

respectively, represent those obtained by using the theory of Ref. [1]. In view of the good agreement between the dashed curves (- - ○ - - and - - + - -) and small differences between the solid curves (— ○ — and — + —), it is believed that the presented theory is reliable. Since the effects of Coriolis force and centrifugal force of the moving mass are neglected in Ref. [1] and they are considered in this subsection, the solid curves are not very close to each other.

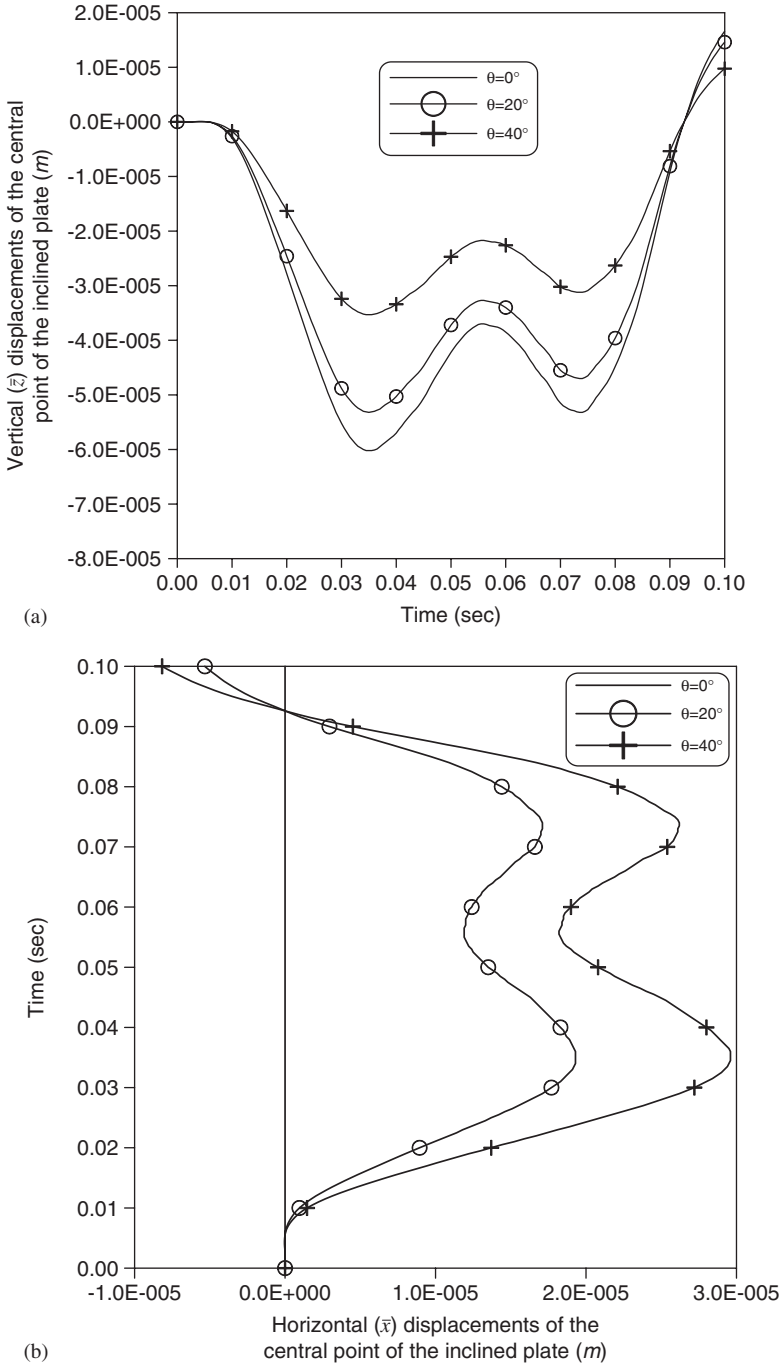

Fig. 6. Influence of inclined angle (θ) on (a) vertical ($\bar{z}$) and (b) horizontal ($\bar{x}$) central displacements of the inclined plate due to a load with $m_c = 2.3\,\text{kg}$ and $V_{cx} = 10.0\,\text{m/s}$.

8.2. Influence of moving-load speed

In this subsection, all conditions for the P–P plate and the moving load are exactly the same as those of the last subsection except that the plate is inclined an angle $\theta = 40^\circ$ (cf. Fig. 4) and the load $m_c = 2.3\,\text{kg}$ moves from the lower-side AB to the upper-side CD of the plate with constant speeds $V_{cx} = 5.0$, 10.0 and 20.0 m/s,

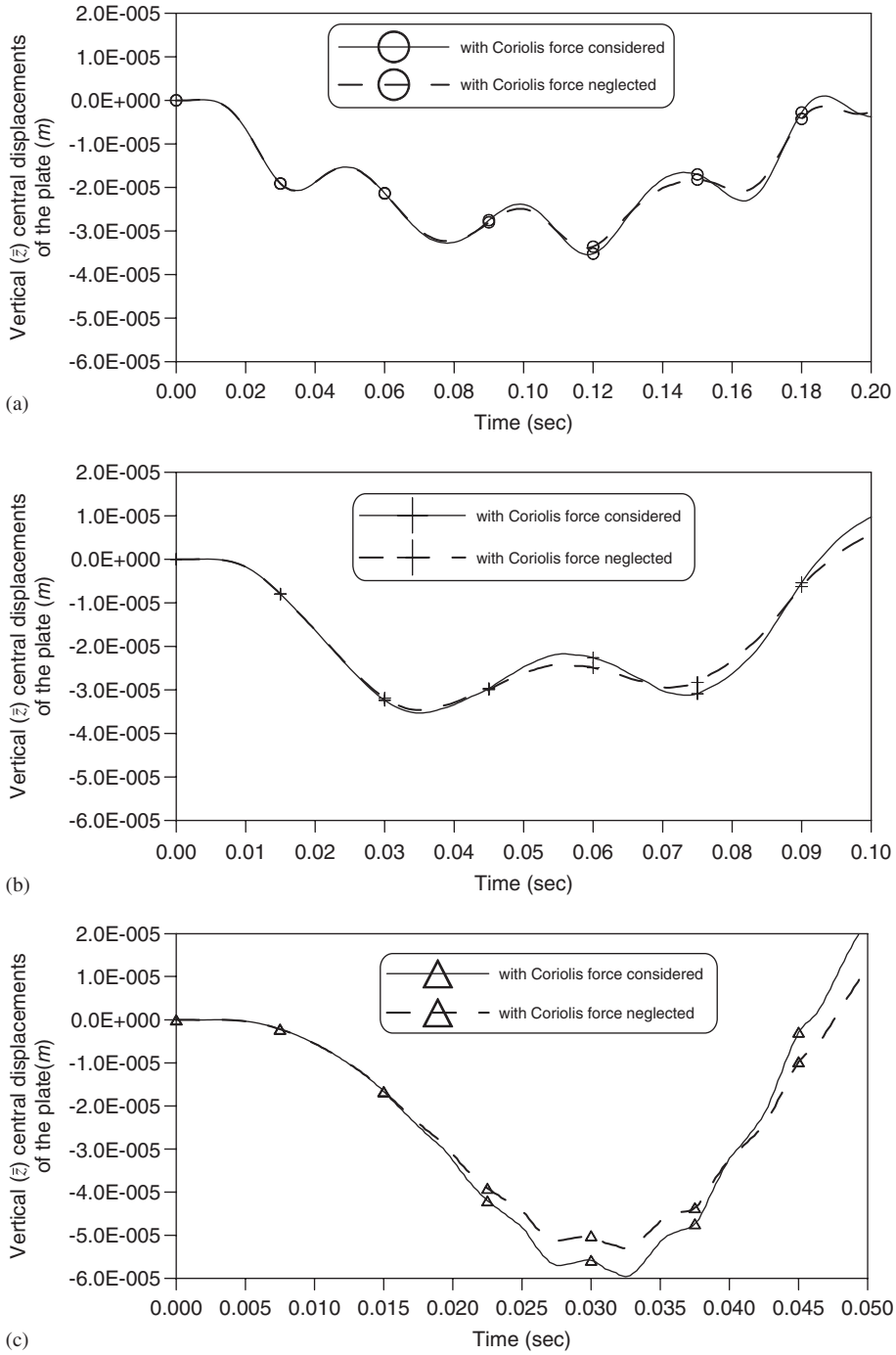

Fig. 7. Influence of Ciriolis force on the vertical ($\bar{z}$) central displacements of the inclined plate ($\theta = 40^\circ$) due to a moving load with $m_c = 2.3\,\text{kg}$ for: (a) $V_{cx} = 5.0\,\text{m/s}$, (b) $V_{cx} = 10.0\,\text{m/s}$ and (c) $V_{cx} = 20.0\,\text{m/s}$.

respectively. The time histories for the vertical ($\bar{z}$) and horizontal ($\bar{x}$) displacements of the central point of the inclined plate are, respectively, shown in Figs. 5(a) and (b). From the figures, one sees that the moving-load speed has significant influence on the maximum vertical ($\bar{z}$) and horizontal ($\bar{x}$) central displacements of the inclined plate.

8.3. Influence of the inclined angle of the plate

Three inclined plates, *iplate0*, *iplate20* and *iplate40*, with inclined angles $\theta = 0^\circ$, 20° and 40°, respectively, are studied here. The load with mass $m_c = 2.3\,\text{kg}$ moves from side AB to side CD of the plate with a constant speed $V_{cx} = 10.0\,\text{m/s}$ (cf., Fig. 4). Figs. 6(a) and (b) show the vertical ($\bar{z}$) and horizontal ($\bar{x}$) central displacements of the plate, respectively. It is seen that the vertical ($\bar{z}$) central displacements of the plate decrease with increasing the inclined angle θ and this trend is reversed for the horizontal ($\bar{x}$) central displacements of the plate.

8.4. Influence of Coriolis force

Since the effect of Coriolis force due to moving mass appears in the damping matrix $[c]$ of the *moving mass element* as seen from Section 2, this effect will disappear if $[c] = [0]$. The same plate as that of the last subsection is investigated here and the vertical ($\bar{z}$) and horizontal ($\bar{x}$) central displacements of the inclined plate are shown in Figs. 7 and 8, respectively. From the last figures, one sees that the influence of Coriolis force on the vertical ($\bar{z}$) and horizontal ($\bar{x}$) central displacements of the inclined plate increases with increasing the moving-load speed. This is because the magnitude of Coriolis force appearing in the damping matrix $[c]$ of the *moving mass element* is proportional to the moving-load speed V (see Eq. 7(c)).

8.5. Influence of centrifugal force

Similarly, one can ignore the effect of centrifugal force due to moving mass by setting the stiffness matrix of the *moving mass element* to be zero, i.e., $[k] = [0]$. The same example as that of the last subsection is investigated and the vertical ($\bar{z}$) and horizontal ($\bar{x}$) central displacements of the inclined plate are shown in

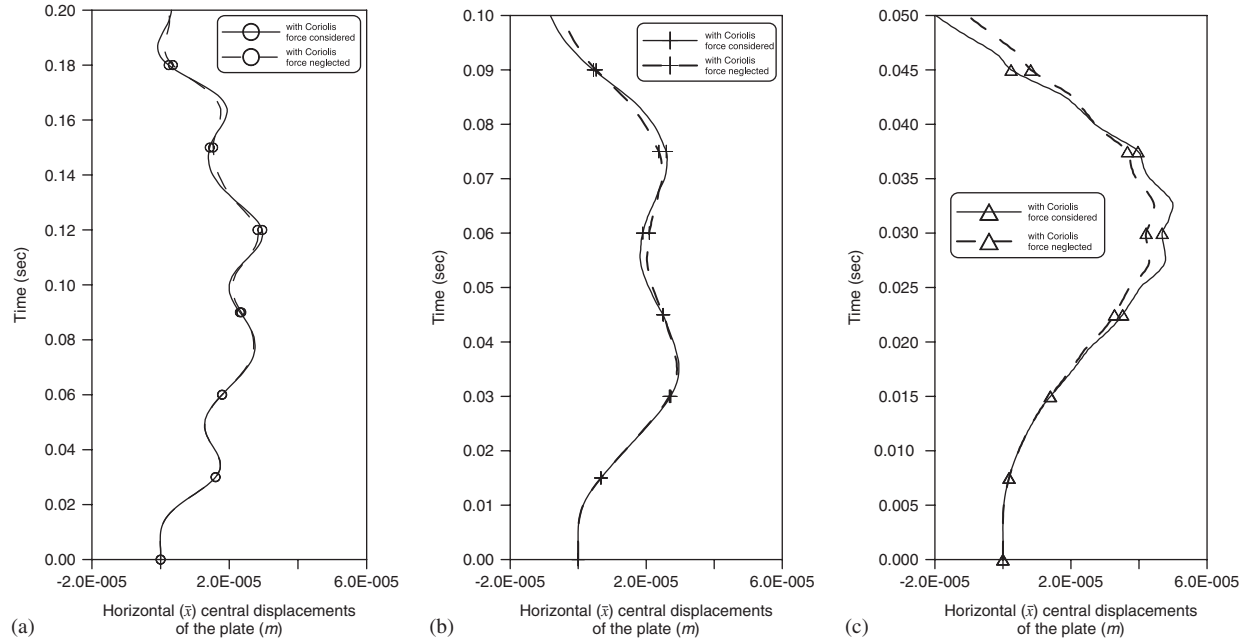

Fig. 8. Influence of Ciriolis force on the horizontal ($\bar{x}$) central displacements of the inclined plate ($\theta = 40^\circ$) due to a moving load with $m_c = 2.3\,\text{kg}$ for: (a) $V_{cx} = 5.0\,\text{m/s}$, (b) $V_{cx} = 10.0\,\text{m/s}$ and (c) $V_{cx} = 20.0\,\text{m/s}$.

Figs. 9 and 10, respectively. From the last two figures, one sees that the influence of centrifugal force on the vertical ($\bar{z}$) and horizontal ($\bar{x}$) central displacements of the inclined plate also increases with increasing the moving-load speed, because the magnitude of centrifugal force appearing in the stiffness matrix [k] of the *moving mass element* is proportional to the moving-load speed (see Eq. (7d)).

8.6. Dynamic responses due to one, two and three moving loads

The dynamic analysis of the *iplate40* subjected to one (m_{c2}), two (m_{c1} and m_{c3}) and three (m_{c1}, m_{c2} and m_{c3}) identical loads and, respectively, moving from the side AB to the side CD of the inclined plate (see Fig. 11) is

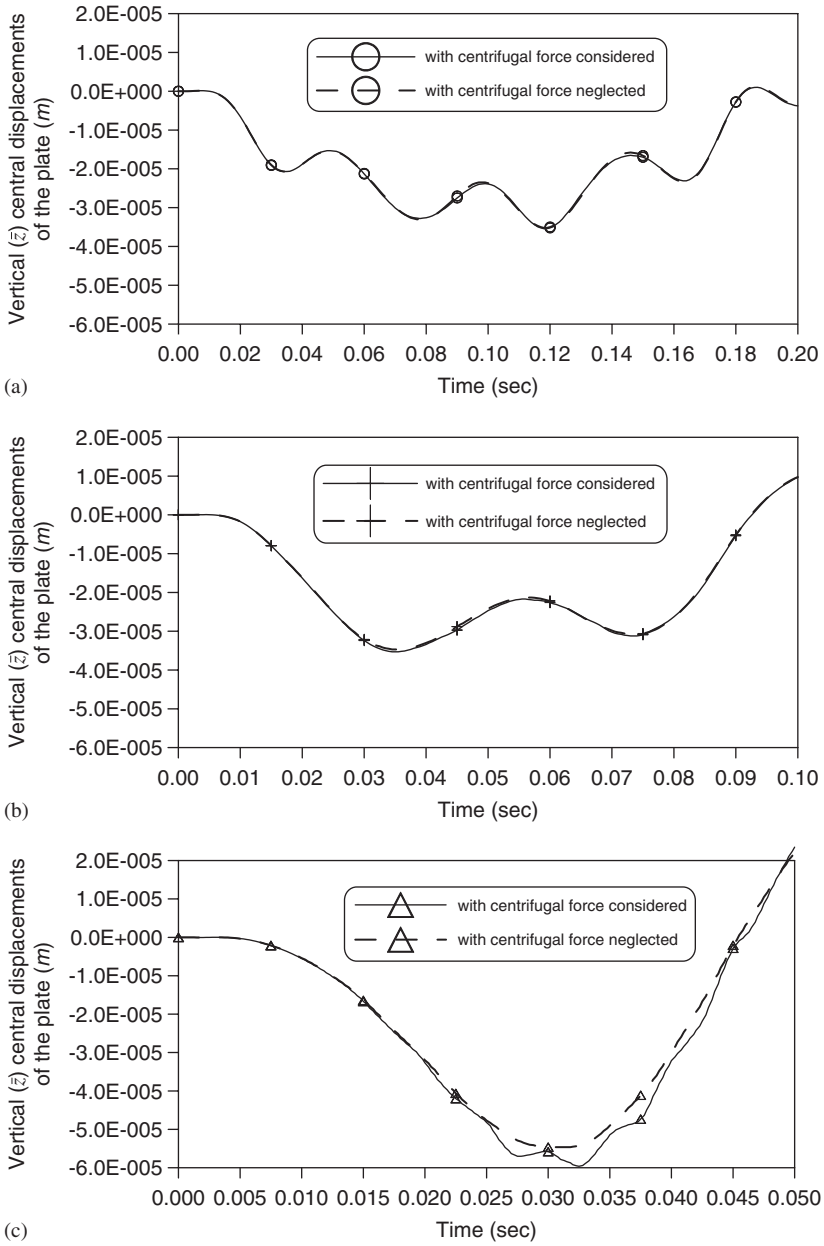

Fig. 9. Influence of centrifugal force on the vertical ($\bar{z}$) central displacements of the inclined plate ($\theta = 40^\circ$) due to a moving load with $m_c = 2.3$ kg for: (a) $V_{cx} = 5.0$ m/s, (b) $V_{cx} = 10.0$ m/s and (c) $V_{cx} = 20.0$ m/s.

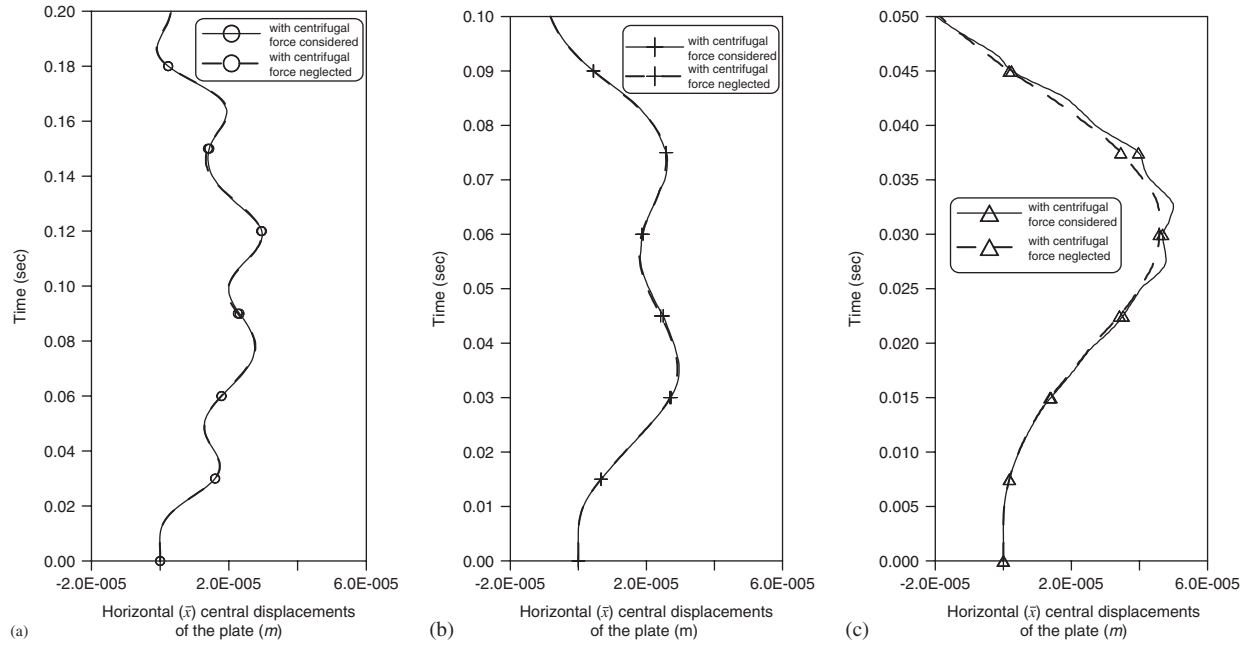

Fig. 10. Influence of centrifugal force on the horizontal ($\bar{x}$) central displacements of the inclined plate ($\theta = 40^\circ$) due to a moving load with $m_c = 2.3\,\text{kg}$ for: (a) $V_{cx} = 5.0\,\text{m/s}$, (b) $V_{cx} = 10.0\,\text{m/s}$ and (c) $V_{cx} = 20.0\,\text{m/s}$.

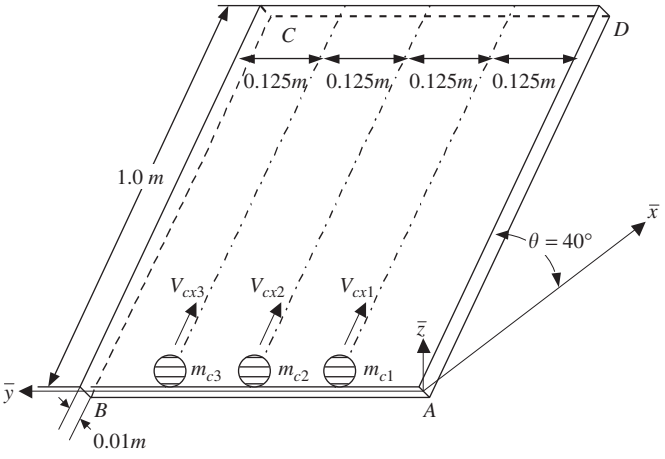

Fig. 11. An inclined P–P plate ($\theta = 40^\circ$) subjected to three concentrated loads ($m_{c1} = m_{c2} = m_{c3} = m_c = 2.3\,\text{kg}$) moving from the lower-side AB to the upper-side CD of the plate with identical speed $V_{cx1} = V_{cx2} = V_{cx3} = V_{cx} = 10.0\,\text{m/s}$.

performed here. For each moving load, the mass is $m_{c1} = m_{c2} = m_{c3} = m_c = 2.3\,\text{kg}$ and the speed is $V_{cx1} = V_{cx2} = V_{cx3} = V_{cx} = 10.0\,\text{m/s}$. The global coordinates for the initial positions of the three moving loads are: $(\bar{x}_{c1}, \bar{y}_{c1}, \bar{z}_{c1}) = (0.0\,\text{m},\ 0.125\,\text{m},\ 0.0\,\text{m})$, $(\bar{x}_{c2}, \bar{y}_{c2}, \bar{z}_{c2}) = (0.0\,\text{m},\ 0.250\,\text{m},\ 0.0\,\text{m})$ and $(\bar{x}_{c3}, \bar{y}_{c3}, \bar{z}_{c3}) = (0.0\,\text{m},\ 0.375\,\text{m},\ 0.0\,\text{m})$, while those for the final positions are: $(\bar{x}'_{c1}, \bar{y}'_{c1}, \bar{z}'_{c1}) = (1.0 \times \cos 40^\circ\,\text{m},\ 0.125\,\text{m},\ 1.0 \times \sin 40^\circ\,\text{m})$, $(\bar{x}'_{c2}, \bar{y}'_{c2}, \bar{z}'_{c2}) = (1.0 \times \cos 40^\circ\,\text{m},\ 0.250\,\text{m},\ 1.0 \times \sin 40^\circ\,\text{m})$ and $(\bar{x}'_{c3}, \bar{y}'_{c3}, \bar{z}'_{c3}) = (1.0 \times \cos 40^\circ\,\text{m},\ 0.375\,\text{m},\ 1.0 \times \sin 40^\circ\,\text{m})$.

Figs. 12(a) and (b), respectively, show the time histories of the vertical ($\bar{z}$) and horizontal ($\bar{x}$) displacements of the central point of the *iplate40*. From the figures, one finds that the ratio between the corresponding dynamic responses of the plate induced by the single moving load (m_{c2}), the two moving loads (m_{c1} and m_{c3}) and the three moving loads (m_{c1}, m_{c2} and m_{c3}) is about 1:2:3. This is a reasonable result, because the ratio

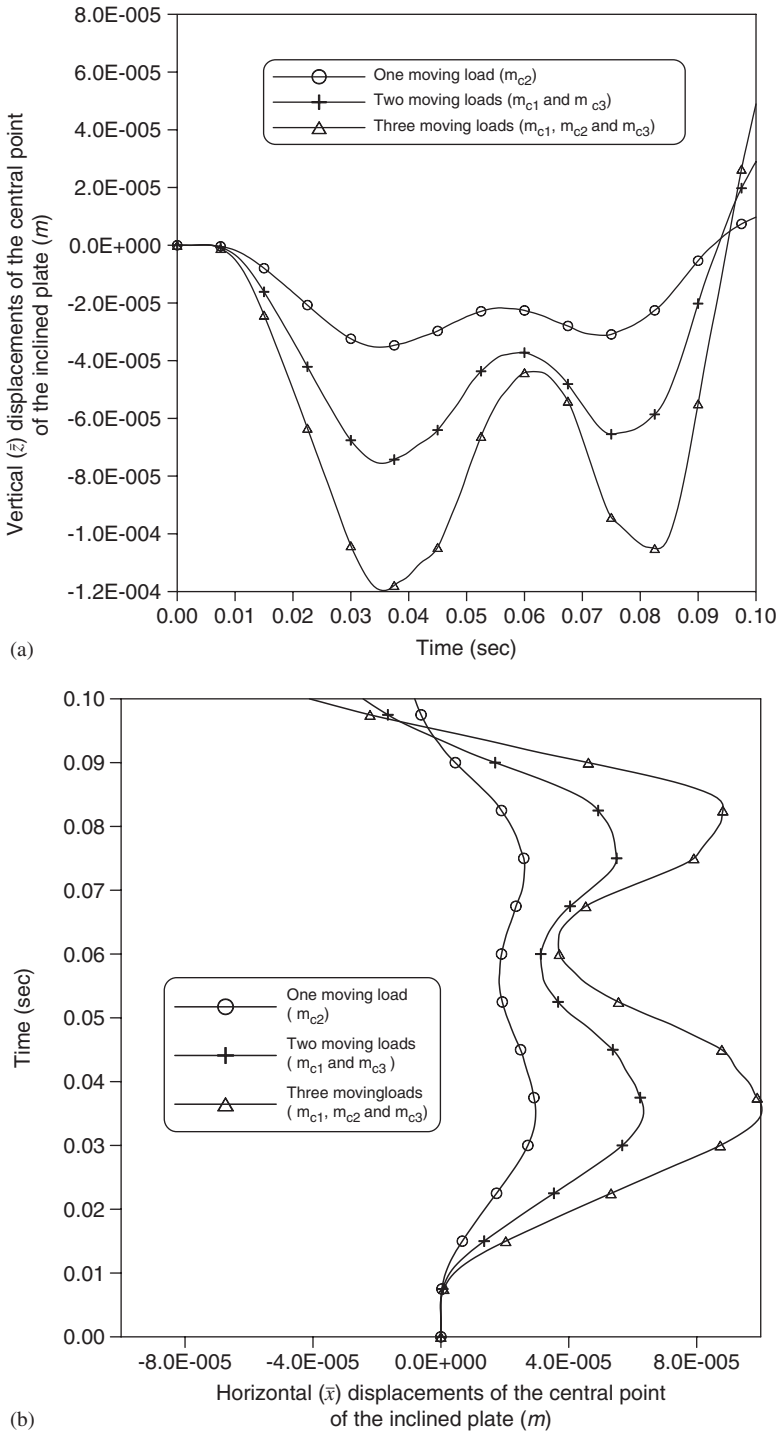

Fig. 12. Time histories for (a) vertical ($\bar{z}$) and (b) horizontal ($\bar{x}$) central displacements of the inclined plate ($\theta = 40^\circ$) subjected to one (m_{c2}), two (m_{c1} and m_{c3}) and three (m_{c1}, m_{c2} and m_{c3}) moving loads, respectively, with $m_{c1} = m_{c2} = m_{c3} = m_c = 2.3\,\text{kg}$ and $V_{cx1} = V_{cx2} = V_{cx3} = V_{cx} = 10.0\,\text{m/s}$.

between the total magnitudes of the moving load(s) for the last three cases is 1:2:3 and the path(s) of the moving load(s) for each case is along or symmetric with respect to the centreline of the inclined plate in the x-direction.

9. Conclusions

Using the theory for *moving mass element* presented in this paper, one can easily study the influence of moving-load-induced inertia force, Coriolis force and centrifugal force on the dynamic behaviour of the inclined plates subjected to moving loads. Numerical results reveal that the influences of moving-load speed, inclined angle of the plate and total number of moving loads on the vertical and horizontal dynamic responses of the inclined plate are significant in most cases, but the effects of Coriolis force and centrifugal force are perceptible only in the case of higher moving-load speed. It has been found that the influences of Coriolis force and centrifugal force on the vertical ($\bar{z}$) and horizontal ($\bar{x}$) central displacements of the inclined plate increase with increasing the moving-load speed.

References

[1] J.S. Wu, M.L. Lee, T.S. Lai, The dynamic analysis of a flat plate under a moving load by the finite element method, *International Journal for Numerical Methods in Engineering* 24 (1987) 743–762.
[2] E. Manoach, Dynamic response of elastoplastic Mindlin plate by mode superposition method, *Journal of Sound and Vibration* 162 (1993) 165–175.
[3] P.K. Chatterjee, T.K. Datta, Dynamic analysis of arch bridges under travelling loads, *International Journal of Solids and Structures* 32 (1995) 1585–1594.
[4] S. Marchesiello, A. Fasana, L. Garibaldi, B.A.D. Piombo, Dynamics of multi-span continuous straight bridges subjected to multi-degrees of freedom moving vehicle excitation, *Journal of Sound and Vibration* 224 (1999) 541–561.
[5] L. Frýba, *Vibration of Solids and Structures under Moving Loads*, Noordhoff International Publishing, The Netherlands, 1971.
[6] J.A. Gbadeyan, S.T. Oni, Dynamic behaviour of beams and rectangular plates under moving loads, *Journal of Sound and Vibration* 182 (1995) 677–695.
[7] J. Renard, M. Taazount, Transient responses of beams and plates subject to travelling load: miscellaneous results, *European Journal of Mechanics—A/Solids* 21 (2002) 301–322.
[8] M.R. Shadnam, F.R. Rofooei, B. Mehri, Dynamics of nonlinear plates under moving loads, *Mechanics Research Communications* 28 (2001) 453–461.
[9] J.J. Wu, Dynamic behaviour of a horizontal rectangular plate undergoing a moving mass, Technique Report, Department of Marine Engineering, National Kaohsiung Institute of Marine Technology, 2003.
[10] R.E. Rossi, R.H. Gutierrez, P.A.A. Laura, Forced vibrations of rectangular plates subjected to harmonic loading distributed over a rectangular subdomain, *Ocean Engineering* 28 (2001) 1575–1584.
[11] H. Takabatake, Dynamic analysis of rectangular plates with stepped thickness subjected to moving loads including additional mass, *Journal of Sound and Vibration* 213 (1998) 829–842.
[12] J.J. Wu, Dynamic analysis of a rectangular plate subjected to multiple forces moving along a circular path, *Journal of Sound and Vibration* 260 (2003) 369–387.
[13] A.V. Kononovm, R. de Borst, Radiation emitted by a constant load in a circular motion on an elastically supported Mindlin plate, *Journal of Sound and Vibration* 245 (2001) 45–61.
[14] J.J. Wu, Dynamic analysis of an inclined beam due to moving loads, *Journal of Sound and Vibration* 288 (2005) 107–131.
[15] R.W. Clough, J. Penzien, *Dynamics of Structures*, McGraw-Hill, New York, 1993.
[16] T.Y. Yang, *Finite Element Structural Analysis*, Prentice-Hall, Englewoods Cliffs, NJ, 1986.
[17] J.S. Przemieniecki, *Theory of Matrix Structural Analysis*, McGraw-Hill, New York, 1985.
[18] K.J. Bathe, *Finite Element Procedures in Engineering Analysis*, Prentice-Hall, Inc., Englewoods Cliffs, NJ, 1982.